Published in final edited form as:
Dev Biol. 2013 May 15; 377(2): 333–344. doi:10.1016/j.ydbio.2013.03.008.

Murine craniofacial development requires Hdac3-mediated repression of *Msx* gene expression

Nikhil Singh[a,1], **Mudit Gupta**[a,1], **Chinmay M. Trivedi**[b], **Manvendra K. Singh**[a], **Li Li**[a], and **Jonathan A. Epstein**[a,*]

[a]Department of Cell and Developmental Biology, Perelman School of Medicine at the University of Pennsylvania, Philadelphia, PA, USA

[b]Department of Medicine, University of Massachusetts Medical School, Worcester, MA, USA

Abstract

Craniofacial development is characterized by reciprocal interactions between neural crest cells and neighboring cell populations of ectodermal, endodermal and mesodermal origin. Various genetic pathways play critical roles in coordinating the development of cranial structures by modulating the growth, survival and differentiation of neural crest cells. However, the regulation of these pathways, particularly at the epigenomic level, remains poorly understood. Using murine genetics, we show that neural crest cells exhibit a requirement for the class I histone deacetylase Hdac3 during craniofacial development. Mice in which Hdac3 has been conditionally deleted in neural crest demonstrate fully penetrant craniofacial abnormalities, including microcephaly, cleft secondary palate and dental hypoplasia. Consistent with these abnormalities, we observe dysregulation of cell cycle genes and increased apoptosis in neural crest structures in mutant embryos. Known regulators of cell cycle progression and apoptosis in neural crest, including Msx1, Msx2 and Bmp4, are upregulated in Hdac3-deficient cranial mesenchyme. These results suggest that Hdac3 serves as a critical regulator of craniofacial morphogenesis, in part by repressing core apoptotic pathways in cranial neural crest cells.

Keywords

Neural crest; Palate development; Cleft palate; Hdac3; Msx1/2; Bmp4

Introduction

Vertebrates are unique among metazoans in their reliance on neural crest cells to form a wide array of head structures. These neural crest-derived craniofacial components are analogous to mesodermally- and ectodermally-derived structures in invertebrates (Gans and Northcutt, 1983). In midgestation in the mouse, neural crest cells populate the pharyngeal arches – a series of paired outpouchings that flank the developing pharynx, as well as the frontonasal prominence, an area that eventually gives rise to the nose and forehead. The first

*Correspondence to: Department of Cell and Developmental Biology, Perelman School of Medicine at the University of Pennsylvania, 1154 BRB II/III, 421 Curie Boulevard, Philadelphia, PA, USA, Office: (215) 898-8731 Fax: (215) 898-9871, epsteinj@upenn.edu (J. Epstein).

[1]These authors contributed equally to this work.

pharyngeal arch, which is the largest and most rostral of the arches, contains the neural crest cells that will form structures in the face and neck (Alappat et al., 2003). Driven by the proliferation and continued influx of migrating neural crest cells, two distinct outgrowths arising from the first arch, known as the maxillary and mandibular prominences, grow ventrally and flank the developing oropharynx, eventually fusing at the ventral midline in what becomes the face. Failure of neural crest cells to migrate or proliferate appropriately can result in hypoplasia of these structures and the absence of fusion, which can manifest as abnormal facies and clefting (Ito et al., 2003; Vallejo-Illarramendi et al., 2009).

In addition to appropriate proliferation and migration, neural crest patterning depends upon carefully controlled apoptosis of premigratory crest cells. In the developing hindbrain, a premigratory neural crest population arises in each of eight rhombomeres. However, the majority of neural crest cells in rhombomeres 3 and 5 undergo apoptosis, and the few surviving cells make small contributions to the discrete streams of migrating neural crest that populate and pattern the developing pharyngeal arches (Graham et al., 1993; Sechrist et al., 1993; Birgbauer et al., 1995; Köntges et al., 1996; Ellies et al., 2002). Loss of this selective apoptosis through ablation of rhombomere 4 causes increased survival and migration of crest cells from rhombomeres 3 and 5, resulting in ectopic muscle attachment sites on the developing mandible (Ellies et al., 2002). A signal for selective apoptosis of neural crest cells specifically in these two rhombomeres is induced by increased expression of *Msx2* (Graham et al., 1994). A related member of this muscle segment homeobox family of genes, *Msx1*, is also a proapoptotic factor in neural crest cells and controls programmed cell death by regulating several caspases in the apoptotic pathway (Tríbulo et al., 2004).

Several human syndromes have implicated *MSX* genes in craniofacial development. Some patients with autosomal-dominant Boston-type craniosynostosis harbor a missense mutation in *MSX2* and present with a variety of malformations including abnormal skull shape and cleft palate (Warman et al., 1993; Jabs et al., 1993). Additionally, deletion of the *MSX1* gene in patients with Wolf-Hirschhorn syndrome manifests with a spectrum of ear, tooth, and skull defects (Ivens et al., 1990). These disorders highlight the critical role that Msx factors play in regulating how the neural crest contributes to the derivative structures that make up the calvaria and face.

Murine genetics have also proven invaluable in deciphering the genetic programs that coordinate the proliferation, migration and apoptosis of cranial neural crest cells. For instance, models of conditional deletion and overexpression of Msx1 and Msx2 have further delineated roles for these molecules in various aspects of craniofacial development. Msx1 has been studied extensively in the developing tooth and is highly expressed in neural crest-derived dental mesenchyme, where it is required for proper condensation and development of the molar tooth germ beyond the bud stage (Satokata et al., 1994; Chen et al., 1996). Deletion of the *Msx1* gene in mice results in reduced *Bmp4* expression in the dental mesenchyme, supporting the well-studied interaction of *Msx* genes and *Bmp4* (Graham et al., 1994; Chen et al., 1996; Bei et al., 2000). In addition to its role in neural crest patterning and apoptosis in the developing hindbrain (Graham et al., 1993, 1994), Msx2 also regulates osteogenesis and functions with Msx1 to control cranial neural crest differentiation into bones of the calvaria (Han et al., 2007; Roybal et al., 2010). Interestingly, both overexpression and inactivation of *Msx2* causes defects in calvaria and tooth development (Dodig et al., 1999; Satokata et al., 2000), suggesting that the Msx1/Msx2 apoptotic pathway must be exquisitely regulated during craniofacial development.

While neural crest proliferation and localized apoptosis are critical for normal craniofacial morphogenesis, little is known about how the pathways controlling these processes are regulated at the epigenetic level. Here, we demonstrate that the class I histone deacetylase

Hdac3 regulates genetic programs involved in murine craniofacial development. Global deletion of *Hdac3* results in lethality prior to E9.5 (Bhaskara et al., 2008). Conditional genetic deletion of *Hdac3* in neural crest results in cleft palate, hypoplastic teeth and a variety of defects in calvarial structures of neural crest origin. Loss of *Hdac3* leads to upregulation of established mediators of neural crest apoptosis, including *Msx1*, *Msx2* and *Bmp4*. These results suggest that Hdac3-mediated repression of Msx signaling plays a critical role in craniofacial development.

Materials and Methods

Mice

Wnt1-Cre, *Pax3*^{Cre}, *Hdac3*^{flox}, *Z/EG* and *p21* null mice were maintained on mixed CD1/B6/129 genetic backgrounds separated by 4–8 generations of interbreeding from pure parental strains (Engleka et al., 2005; Jiang et al., 2000; Mullican et al., 2011; Novak et al., 2000). Mice were genotyped using previously described Cre-specific PCR primers (5′-TGC CAC GAC CAA GTG ACA GC-3′, 5′-CCA GGT TAC GGA TAT AGT TCA TG-3′) (Heidt and Black, 2005), and primers designed to distinguish between the control and floxed *Hdac3* allele (5′-GCA GTG GTG GTG AAT GGC TT-3′, 5′-CCT GTG TAA CGG GAG CAG AAC TC-3′). Genotyping for the Z/EG transgene was performed by X-Gal staining tail samples. Littermate embryos were analyzed in all experiments unless otherwise noted. The University of Pennsylvania Institutional Animal Care and Use Committee approved all animal protocols.

Histology, immunohistochemistry and in situ hybridization

These techniques were performed on paraformaldehyde-fixed, paraffin embedded slides as previously described (High et al., 2008). Embryos were dissected in cold PBS, fixed overnight in 2% paraformaldehyde, dehydrated into 100% ethanol, embedded in paraffin and sectioned. H&E and Goldner's trichrome staining were performed using standard procedures. Primary antibodies used for immunohistochemistry were anti-GFP goat polyclonal (Abcam ab6673, 1:100), anti-GFP rabbit polyclonal (Invitrogen A-11122, 1:200), anti-Runx2 rabbit polyclonal (Santa Cruz sc-10758, 1:20), anti-phospho-histone H3 rabbit polyclonal (Cell Signaling #9701, 1:50) and anti-Hdac3 rabbit polyclonal (Santa Cruz sc-11417x, 1:10). Radioactive *in situ* hybridization for *Msx1,Msx2* and *PlexinA2* was performed as previously described (Engleka et al., 2005). *Msx1* probe corresponds to RefSeq #NM_010835 (bp 862-1741), *Msx2* to #NM_013601 (bp 159-1143) and *PlexinA2* as previously described (Brown et al., 2001). TUNEL staining was performed as previously described (Jain et al., 2011). All control and mutant histological and immunohistochemical images shown for comparison were taken at the same exposure and contrast settings, using NIS Elements software. Pharyngeal arch size was quantified using ImageJ software by counting number of pixels in at least three serial sections from control and mutant frontal sections. All quantification was done in a blinded manner.

Cell number, proliferation and apoptosis were quantified by manually counting nuclei, phospho-histone H3-, or TUNEL-positive cells, respectively, in adjacent sections of the anatomically-defined palatal shelf region in a blinded manner.

Optical projection tomography

Samples were dehydrated into 100% methanol, embedded in 1% low-melt agarose, cleared overnight in 1:2 (v/v) benzyl alcohol and benzyl benzoate, and scanned using the Bioptonics OPT scanner (3001M) (Sharpe et al., 2002). Image stacks were reconstructed using OsiriX software. Image contrast was optimized to show anatomic detail.

siRNA transfection

E12.5 anterior craniofacial mesenchyme was microdissected and dissociated to single cell suspension with 0.25% Trypsin-EDTA. Cells were incubated at 37 degrees C in 5% CO_2 for 16 hours before transfection with 50nM control (Santa Cruz sc-37007), Msx1 (Dharmacon #M-044089-01) or Msx2 siRNA (Dharmacon #M-047845-01) using Lipofectamine RNAiMax (Invitrogen #13778030). 24 hours after transfection, cells were fixed with 4% paraformaldehyde (10 min, room temperature) and permeabilized with 0.2% Triton X-100. Immunocytochemistry was performed with anti-phospho-histone H3 rabbit polyclonal (Cell Signaling #9701, 1:100). Cell number and proliferation were quantified by manually counting nuclei and phospho-histone H3-positive cells in a blinded manner.

Alcian blue/alizarin red staining

Neonatal mice were eviscerated and skinned after being soaked in room temperature water for 3 hours followed by a 1 minute heat shock at 65 degrees C to loosen the skin. The samples were then fixed for 3 days in 100% ethanol at room temperature. Samples were stained for 2 days at room temperature with Alcian blue solution (0.3mg/ml Alcian Blue, 80% ethanol, 20% acetic acid) to visualize cartilage, and then rinsed and postfixed in 100% ethanol at room temperature, overnight. Samples were then incubated for 24 hours with Alizarin Red solution (0.065mg/ml Alizarin Red S in 0.5% KOH) to visualize bone, followed by incubation in 0.5% KOH until soft tissues were mostly digested. The 0.5% KOH solution was replaced with 25% glycerol in water (added very slowly to sample) and incubated at room temperature until tissues cleared.

RNA isolation, complementary DNA synthesis and quantitative RT-PCR

For E12.5 cranial mesenchyme expression profiling, *Wnt1-Cre; Hdac3*$^{f/f}$ and littermate Cre-negative control embryos were microdissected with tungsten needles in cold PBS. RNA was obtained using the Qiagen RNeasy spin column, with on-column DNAse I digestion. Complementary DNA (cDNA) was synthesized according to kit instructions with the Superscript III system (Invitrogen). Quantitative RT-PCR was performed in triplicate using SYBR Green (Applied Biosystems). *Gapdh* was used as a reference control gene. Quantitative RT-PCR primers (Table S1) were designed using IDT software.

Statistics

The student's two-tailed t test was used to ascertain differences between groups. A p-value of less than 0.05 was considered significant.

Results

Hdac3 is widely expressed during craniofacial development and is efficiently deleted in neural crest derivatives by Wnt1-Cre

In order to explore the epigenomic regulation of craniofacial development, we deleted the class I histone deacetylase *Hdac3* in premigratory neural crest cells using the *Wnt1-Cre* transgene and a floxed *Hdac3* allele (*Hdac3*^{f}) (Jiang et al., 2000; Mullican et al., 2011). Using the Z/EG reporter allele (Novak et al., 2000), we observed that both *Wnt1-Cre; Hdac3*$^{f/f}$ (which we have termed *Hdac3*^{Wnt1NCKO}*); Z/EG* and *Wnt1-Cre; Z/EG* control embryos demonstrate intact migration of neural crest cells into the developing face and pharyngeal arch region at E9.5 (Fig. 1A and Supplemental Fig. 1). Immunohistochemistry of staged embryos demonstrates that Hdac3 is widely expressed in the developing head at E9.5 and E10.5, including in neural crest, ectoderm and endoderm (Fig. 1B and data not shown). Expression of *PlexinA2*, a neural crest marker (Brown et al., 2001), appears unaltered in *Hdac3* mutant embryos at E9.5 (Supplemental Fig. 1), further indicating that neural crest

migration is normal at this stage. In *Hdac3*^{Wnt1NCKO} embryos, Hdac3 protein expression is lost in neural crest-derived craniofacial mesenchyme, while expression is retained in ectoderm and endoderm (Fig. 1B). In the absence of neural crest expression of Hdac3, the maxillary and mandibular prominences of the first pharyngeal arch demonstrate mild hypoplasia as early as E10.5 (Figs. 1B and C). This is in contrast to the caudal pharyngeal arches, which demonstrate no hypoplasia at E10.5 in the absence of Hdac3 expression (Singh et al., 2011).

Hdac3^{Wnt1NCKO} embryos exhibit severe craniofacial abnormalities in late gestation, resulting in perinatal lethality

Embryos in which Hdac3 is deleted in neural crest cells are found at expected Mendelian ratios in late gestation and are viable until birth, but uniformly succumb at P0 (Singh et al., 2011). *Hdac3*^{Wnt1NCKO} mice are born with microcephaly, micrognathia, a shortened snout and eyelid closure defects, with preservation of body morphology (Fig. 2A). Optical projection tomography and histology of *Hdac3*^{Wnt1NCKO} P0 heads reveals cleft palate, which is also apparent in late gestation embryos (Figs. 2B and C). The palate defect is characterized by a large posterior cleft, without additional facial clefting (Fig. 2 B). Cleft palate is fatal in perinatal mice; afflicted pups are unable to generate suction and nurse, and subsequently die at P0 from dehydration and accumulation of air in the digestive tract (Condie et al., 1997; Qiu et al., 1995). Consistent with these reports, *Hdac3*^{Wnt1NCKO} pups are unable to feed, as evidenced by the lack of a milk spot (Fig. 2A). The gross craniofacial defects observed in *Hdac3*^{Wnt1NCKO} mice are fully penetrant and are summarized in Table 1. We observed similar craniofacial abnormalities using a second neural crest driver, *Pax3*^{Cre} (Engleka et al., 2005); these abnormalities are also fully penetrant both at P0 and in late gestation (Supplemental Fig. 2 and unpublished observations).

Loss of Hdac3 in neural crest leads to bone defects in the calvaria and viscerocranium

In the adult vertebrate, osteoblasts are among the most abundant cell types generated by cranial neural crest. These neural crest-derived osteoblasts contribute to the bones of the face, the skull base and the entirety of the calvaria, with the exception of the parietal bone (Santagati and Rijli, 2003). Hdac3 has previously been implicated in multiple stages of osteoblast differentiation and maturation. In committed, undifferentiated osteoblasts that express the *Osx-Cre* transgene, deletion of Hdac3 leads to subtle abnormalities in calvarial osteoblast differentiation, and progressive abnormalities in trabecular bones that lead to perinatal runting and death early in adulthood (Razidlo et al., 2010).

Consistent with a pro-osteogenic role for Hdac3 at the earliest stages of bone development in neural crest, *Hdac3*^{Wnt1NCKO} mice - in which Hdac3 is deleted prior to osteoblast specification (before the onset of *Osx-Cre* expression) - exhibit severe bone defects in the calvaria and viscerocranium (Fig. 3). Alcian blue/alizarin red staining of the late embryonic and perinatal mice reveals decreased ossification of the calvaria, particularly in the region of the frontal bone, where ossified bone is nearly undetectable by alizarin red staining (Fig. 3A). The open frontal fontanel leads to hemorrhage in some newborn pups following parturition (Fig. 2B). The parietal bone develops normally in *Hdac3*^{Wnt1NCKO} mutants, consistent with its mesodermal origin (Fig. 3A). In mutant embryos, ossification abnormalities of the viscerocranium were also identified in the mandible, skull base and tympanic ring (Fig. 3A).

Additional bone abnormalities in E17.5 mutant embryos are detectable by Goldner's trichrome staining. Neural crest-derived calvarial bones, including the frontal bone, are thin and show minimal mineralization (Fig. 3B). Additionally, at variable penetrance, absence of ossification in the sphenoid bone plate results in encephalocoele, in which the brain

herniates into the nasal sinuses (Fig. 3B). The bone defects observed in *Hdac3*^{Wnt1NCKO} mice are summarized in Table 1.

To establish whether loss of *Hdac3* in the developing calvaria affects migration and survival of neural crest, or differentiation of osteogenic precursors, we fate mapped cranial crest cells to the E12.5 calvaria using the Z/EG reporter, measured apoptosis with TUNEL staining and evaluated pre-osteoblast differentiation by Runx2 immunohistochemistry (Supplemental Fig. 3). We observed that mutant cranial crest exhibit normal migration to the calvaria and normal expression of the critical ossification regulator Runx2 at the frontal bone primordium (Ishii et al., 2003), but demonstrate increased apoptosis compared to controls. These observations suggest that the bone abnormalities in the *Hdac3*^{Wnt1NCKO} mice are associated with decreased survival of neural crest cells, and are unlikely to be due to a primary abnormality in differentiation or migration.

Hdac3 is required for normal odontogenesis

Seminal work in amphibians and avian models established that the cranial neural crest makes up a significant portion of the developing tooth, specifically the dental mesenchyme (LeDouarin, 1982; reviewed by Maas and Bei, 1997). Further studies in mouse demonstrate that patterning of the developing molar tooth germ is influenced by the interaction of the epithelium and mesenchyme. Recombination experiments with neural crest and epithelium revealed that early (E9.5-12.0) oral epithelium can signal to non-dental mesenchyme to form teeth; however, later in development, the dental mesenchyme possesses odontogenic potential to induce non-oral epithelium to become enamel (Kollar et al., 1969; Mina et al., 1987; Lumsden 1988).

In murine tooth development, signals from the epithelium initiate condensation of neighboring mesenchyme composed of neural crest cells at E11.5 (Chen et al., 2000). As epithelial cells invaginate, they envelop neural crest cells, which will eventually form the pulp of the tooth (Fig. 4A). In *Hdac3*^{Wnt1NCKO} embryos, the early stages of odontogenesis proceed normally, with tooth bud morphology at E15.5 appearing similar to littermate controls through the bud and cap stages (Figs. 4 A–D). However, expansion of the neural crest-derived mesenchyme does not occur between E15.5-E17.5, resulting in hypoplastic teeth with the absence of normal pitting (Figs. 2C, 4E and F). The tooth bud hypoplasia in mutant embryos parallels the hypoplasia observed in other neural crest-derived structures in late gestation (Fig. 2).

Aberrant cell cycle regulation in Hdac3-deficient cranial mesenchyme leads to a failure of neural crest cell expansion, dental hypoplasia and cleft palate

In order to further delineate the mechanism by which deletion of *Hdac3* results in hypoplasia of neural crest structures, we performed a histological analysis of staged control versus *Hdac3*^{Wnt1NCKO} embryos. In normal palatogenesis, the anterior palate is formed by fusion of the maxillary prominence with the frontonasal prominence. *Hdac3*^{Wnt1NCKO} embryos exhibit posterior cleft palate, suggesting that secondary palatogenesis is disrupted (Fig. 2B). The posterior aspects of the hard palate (referred to as the secondary palate) are formed from two outgrowths of neural crest-derived mesenchyme that lie on either side of the stomodeum. These outgrowths - the palatal shelves - are detectable at E11.5 in the mouse at both anterior and posterior levels (Figs. 5A and A′). Between E11.5 and E13.5, the palatal shelves, driven by neural crest cell proliferation, expand towards the mandible (Figs. 5A, A′, B and B′). Between E13.5 and E14.5 the palatal shelves elevate relative to the tongue and fuse in the midline with the nasal septum (Figs. 5C and C′). This newly formed structure subsequently ossifies, giving rise to the mature secondary palate (Figs. 5D and D′).

Disruption of any of the stages of secondary palatogenesis - palatal shelf formation, expansion, elevation, fusion or ossification – can lead to cleft palate in mice, and similar mechanisms are believed to contribute to secondary cleft palate in humans (He et al., 2011; Ito et al., 2003; Richarte et al., 2007; Vallejo-Illarramendi et al., 2009; Wu et al., 2008). Histological analysis of *Hdac3*^{Wnt1NCKO} embryos reveals that the palatal shelves form appropriately but are hypoplastic at E12.5 (Figs. 5 E, E′, F and F′). Despite appropriate elevation of the medial aspect of the palatal shelves by E14.5, the palatal shelves do not meet at the midline (Figs. 5G and G′). These results suggest that cleft palate in *Hdac3*^{Wnt1NCKO} embryos is due to a failure of palatal shelf expansion.

Expansion of the palatal shelves is dependent upon proliferation and survival of the neural crest cells that make up the palatal shelf mesenchyme (Ito et al., 2003). In E12.5 mutant versus control palatal shelves that were matched for surrounding anatomical landmarks, we detected a significant increase in apoptosis and a trend towards decreased proliferation, as determined by TUNEL and phospho-histone H3 staining, respectively (Fig. 5I). Increased TUNEL staining is also visible throughout additional cranial neural crest-derived structures outside of the palatal shelf region including the tooth bud and calvaria, suggesting that hypoplasia of these structures is also mediated by increased apoptosis (Figs. 5I, 6E and Supplemental Fig. 3).

To discern the nature of the cell cycle dysregulation in *Hdac3*^{Wnt1NCKO} cranial mesenchyme, we performed expression profiling by quantitative RT-PCR of microdissected anterior cranial tissue of E12.5 mutant embryos and littermate controls (Fig. 6A). While *Hdac3* expression in mutant tissue is significantly downregulated, expression of the other class I Hdacs is unchanged (Fig. 6B). Strikingly, the expression of multiple cell cycle regulators is altered in *Hdac3*^{Wnt1NCKO} cranial mesenchyme. *Cdkn1a* (*p21*), *Trp53* (*p53*), *Cdkn1c* (*p57*), *Ccnd1* (*Cyclin D1*), *Ccnd3* (*Cyclin D3*), *CcnG1* (*Cyclin G1*) and *Cdk2* are significantly upregulated in the absence of Hdac3, while *Cdkn2c* (*p18*) expression is downregulated (Fig. 6C). This pattern of gene dysregulation is consistent with G1/S arrest of neural crest cells.

Hdac3 has previously been shown to directly repress the cell cycle inhibitor gene *Cdkn1a* (p21) in multiple tissues (Trivedi et al., 2008; Wilson et al., 2008). In order to determine whether the substantial upregulation of *Cdkn1a* observed in *Hdac3*^{Wnt1NCKO} cranial mesenchyme is sufficient to account for cleft palate and microcephaly in these embryos, we deleted *Hdac3* in neural crest on a *Cdkn1a* null background (Deng et al., 1995). Homozygous *Cdkn1a*$^{-/-}$ mice develop normally and are viable and fertile (Deng et al., 1995). We found that loss of *p21* does not rescue the cleft palate and microcephaly observed in *Hdac3*^{Wnt1NCKO} embryos, suggesting that dysregulation of additional cell cycle modulators contributes to altered regulation of neural crest expansion in *Hdac3*-deficient cranial neural crest cells, and ultimately to cleft palate and craniofacial hypoplasia (Supplemental Fig. 4).

The loss of Hdac3 results in dysregulation of core networks that regulate craniofacial development

In multiple aspects of embryogenesis, including neural crest development and limb development, the homeobox transcription factors Msx1 and Msx2 and the signaling molecule Bmp4 function to initiate apoptosis (Barlow and Francis-West, 1997; Graham et al., 1994; Lallemand et al., 2005; Marazzi et al., 1997). Msx1 is expressed in the palatal shelves and dental mesenchyme, and regulates development of these neural crest-derived structures (Satokata et al., 1994; Chen et al., 1996; Maas and Bei, 1997; Bei et al., 2000; Alappat et al., 2003). Msx2 is expressed in the early dental mesenchyme and is also crucial for normal tooth development (Maas and Bei, 1997; Winograd et al., 1997). Bmp4 is

primarily expressed by epithelial structures in the developing face, which signal to neural crest-derived mesenchyme to mediate processes such as palatogenesis and odontogenesis, and its expression can be induced by Msx genes in neural crest derivatives (Zhang et al., 2002, Mitsiadis et al., 2010).

We measured the expression of important regulatory genes involved in craniofacial development using a candidate approach, and detected significant upregulation of *Msx1*, *Msx2* and the target gene *Bmp4* in the anterior cranial mesenchyme of E12.5 $Hdac3^{Wnt1NCKO}$ embryos, but found no significant differences in the expression of palate-specific markers *Osr2* and *Shox2* (Fig. 6D and Supplemental Fig. 5) (Lan et al., 2004; Yu et al., 2005). *In situ* hybridization reveals substantially more expression of *Msx1* transcripts in the dental mesenchyme of mutant embryos than in littermate controls (Fig. 6E). We also observe increased expression of *Msx1* in the developing palatal shelves of *Hdac3*-deficient embryos compared to littermate controls (Fig. 6F). Similar to *Msx1*, *in situ* hybridization for *Msx2* shows elevated expression specifically in the dental mesenchyme of E12.5 $Hdac3^{Wnt1NCKO}$ embryos (Fig. 6E).

Interestingly, transgenic overexpression of *Msx2* leads to cleft secondary palate, skull malformations, micrognathia, tooth hypoplasia and eyelid dysplasia, which phenocopies many aspects of the $Hdac3^{Wnt1NCKO}$ abnormalities (Winograd et al., 1997). Gain of BMP signaling also results in craniofacial abnormalities that partially phenocopy the abnormalities identified in $Hdac3^{Wnt1NCKO}$ embryos (He et al., 2010). These observations suggest that the hypoplasia of neural crest-derived structures observed in $Hdac3^{Wnt1NCKO}$ embryos may be in part mediated by derepression of *Msx1* and *Msx2* leading to increased apoptosis (Graham et al., 1994; Tríbulo et al., 2004; Park et al., 2005). Consistent with this hypothesis, we observed increased apoptosis in *Hdac3* mutants in dental mesenchyme and palatal shelves, coincident with increased *Msx* expression (Figs. 6E and F).

To determine whether *Msx* gene upregulation has a functional role in mediating the observed cell cycle dysregulation and failure of neural crest structures to expand during development, we performed siRNA-mediated knockdown of *Msx1* or *Msx2,* individually or in combination, in cultured neural crest mesenchyme from control and $Hdac3^{Wnt1NCKO}$ embryos. We observed a partial restoration of wild-type levels of neural crest proliferation following knockdown of either *Msx1* or *Msx2* (Supplemental Fig. 6). Taken as a whole, these results suggest that derepression of *Msx1* and *Msx2* in the absence of Hdac3 causes decreased proliferation and increased apoptosis in cranial neural crest cells, manifesting as abnormal facies, cleft palate, dental hypoplasia and bone deficiencies.

In addition to the *Msx* gene products, the T-box transcription factors Tbx2 and Tbx3 have been shown to play significant roles in palate expansion and neural crest development (Zirzow et al., 2009; Mesbah et al., 2012). Tbx2 and Tbx3, like Msx1 and Msx2, are normally expressed in neural crest-derived cranial mesenchyme and are important in cell cycle regulation during palatogenesis (Zirzow et al., 2009). Loss of *Tbx2* or *Tbx3* in craniofacial development leads to cleft palate due to excessive proliferation, and both proteins have been identified as inhibitors of the cell cycle in palatogenesis (Zirzow et al., 2009). We observe significant upregulation of these members of the T-box transcription factor family in *Hdac3*-deficient craniofacial mesenchyme, consistent with the observed cell cycle dysregulation in neural crest-derived tissue (Fig. 6D). Overall, the pattern of upregulation of these Msx, T-box transcription factors, cell cycle regulators and the signaling molecule Bmp4 – all known inhibitors of neural crest survival - is consistent with a model in which Hdac3 represses core inhibitors of the neural crest cell cycle in order to drive craniofacial development.

Discussion

At multiple stages of neural crest development, the growth and survival of neural crest cells comes under positive and negative regulation from surrounding cell types, but is also subject to cell autonomous regulation (Sauka-Spengler and Bronner-Fraser, 2008). The homeodomain transcription factors Msx1 and Msx2 are important mediators of neural crest apoptosis in both early and late stages of craniofacial morphogenesis, but the temporal and spatial regulation of their expression is poorly understood. Interestingly, both increased and decreased *Msx* gene levels in developing neural crest lead to severe craniofacial abnormalities (Bei and Maas, 1998; He et al., 2010). That craniofacial morphogenesis is so exquisitely sensitive to *Msx* expression speaks to the importance of fine regulation of the timing and patterning of *Msx1* and *Msx2* transcription during neural crest development.

In this study, we have demonstrated that loss of *Hdac3* in neural crest results in severe craniofacial malformations including microcephaly, cleft palate, impaired bone formation in the skull and hypoplasia of the teeth. Inactivation of *Hdac3* by *Wnt1-Cre* results in cell cycle dysregulation in neural crest-derived structures, including increased expression of *p21, p53, p57, Cyclin D1, Cyclin D3, Cyclin G1 and Cdk2. Hdac3*^{Wnt1NCKO} embryos exhibit elevated expression of *Msx1* and *Msx2* in the anterior cranial mesenchyme, and knockdown of *Msx1* and *Msx2* in mutant tissue partially normalizes neural crest proliferation. Incomplete rescue in this assay may have been due to incomplete knockdown of *Msx1* and *Msx2* using siRNA approaches, but may also suggest that factors other than *Msx1* and *Msx2* are functionally altered in *Hdac3* mutants and contribute to the cell cycle dysregulation that we observe. Indeed we observe upregulation of *Tbx2* and *Tbx3* in *Hdac3*-deficient cranial mesenchyme, and abnormal T-box factor expression is also likely to contribute to the abnormal phenotype in *Hdac3*^{Wnt1NCKO} mice. Dysregulation of Tbx factors and other regulators of neural crest development is also likely to explain the strong – but not complete – overlap between the phenotype of *Hdac3*^{Wnt1NCKO} mice and *Msx2* transgenic overexpressing mice (Winograd et al., 1997).

Previous work investigating the regulation of *Msx1* transcription in cell lines identified several regulatory elements in the *Msx1* upstream genomic region (Takahashi et al., 1997). *LacZ* reporters of a “minimal” *Msx1* promoter containing these regulatory regions were strongly expressed in the neural crest-derived anterior cranial mesenchyme of E12.5 embryos (Takahashi et al., 1997). Similar work with the *Msx2* promoter region has also identified highly conserved enhancers that contribute to *Msx2* expression in the craniofacial mesenchyme when fused to *lacZ* reporters (Liu et al., 1994). In light of the canonical role of Hdac3 as a transcriptional repressor, it is reasonable to hypothesize that Hdac3 may directly repress *Msx1* and *Msx2* expression in neural crest by deacetylating histones at these promoters/enhancers, either at known or novel regulatory regions. However, our *in vivo* chromatin immunoprecipitation experiments have not demonstrated Hdac3 occupancy of previously described enhancer regions (Brugger et al., 2004; Hussein et al., 2003). As a global modulator of gene expression, Hdac3 is likely to affect the expression of multiple pathways involved in craniofacial development. Additional work is needed to determine whether Hdac3-mediated repression of *Msx1* and *Msx2* occurs via histone deacetylation at uncharacterized enhancer regions at these loci, through derepression of additional intermediate genes or via direct deacetylation of non-histone targets. Interestingly, recent results suggest that critical functions of Hdac3 in the embryo are independent of its interactions with NCOR1 and SMRT, co-repressors that are necessary for Hdac3 catalytic activity (You et al., 2013). Thus, Hdac3 may mediate important developmental processes through a non-canonical function unrelated to deacetylation of histone targets.

Our finding of decreased bone formation in Hdac3 conditional mutants is consistent with the pro-ossification role that Hdac3 is known to play in osteoblast precursors; however, by deleting *Hdac3* prior to the specification and expansion of osteoblast precursors, we observe drastic deficiencies in bone formation not seen after deletion of *Hdac3* in committed *Osx*-expressing cells (Razidlo et al., 2010). Our results demonstrate increased apoptosis of neural crest-derived mesenchyme in the developing calvaria, despite intact neural crest migration and normal expression of the osteoblast regulatory molecule Runx2. Paradoxically, deletion of *Msx1* and *Msx2* in neural crest leads to heterotopic bone formation, particularly in the frontal bone region, while *Msx2* transgenic overexpression also results in ectopic bone formation, with decreased mineralization in the interparietal bone (Liu et al., 1995; Roybal et al., 2010; Winograd et al., 1997). While some of the bone abnormalities in $Hdac3^{Wnt1NCKO}$ embryos could be attributed to derepression of *Msx* gene expression, it is likely that additional targets of Hdac3 underlie the skeletal abnormalities in these mice. An interesting future area of research will involve determining additional targets of Hdac3 that regulate the early stages of bone development in neural crest progenitor cells and additional populations of osteoblast precursors.

Supplementary Material

Refer to Web version on PubMed Central for supplementary material.

Acknowledgments

This work was supported by R01 HL071546, the WW Smith endowed chair, and the Spain Fund for Cardiovascular Research (J.A.E.), the Medical Scientist Training Program grant (N.S., M.G.), T32 HL007954-13 (M.G.) and K99-R00 HL098366 (C.M.T). We would like to acknowledge Ashley Cohen for animal husbandry and Kurt Engleka for OPT imaging and data analysis. We would also like to thank Mitch Lazar, Theresa Alenghat and Shannon Mullican for generously providing us with the Hdac3 floxed mice.

References

Alappat S, Zhang ZY, Chen YP. Msx homeobox gene family and craniofacial development. Cell Res. 2003; 13:429–442. [PubMed: 14728799]

Barlow AJ, Francis-West PH. Ectopic application of recombinant BMP-2 and BMP-4 can change patterning of developing chick facial primordia. Development. 1997; 124:391–398. [PubMed: 9053315]

Bei M, Maas R. FGFs and BMP4 induce both Msx1-independent and Msx1-dependent signaling pathways in early tooth development. Development. 1998; 125:4325–4333. [PubMed: 9753686]

Bei M, Kratochwil K, Maas RL. BMP4 rescues a non-cell-autonomous function of Msx1 in tooth development. Development. 2000; 127:4711–8. [PubMed: 11023873]

Bhaskara S, Chyla BJ, Amann JM, Knutson SK, Cortez D, Sun ZW, Hiebert SW. Deletion of histone deacetylase 3 reveals critical roles in S phase progression and DNA damage control. Mol Cell. 2008; 30:61–72. [PubMed: 18406327]

Birgbauer E, Sechrist J, Bronner-Fraser M, Fraser S. Rhombomeric origin and rostrocaudal reassortment of neural crest cells revealed by intravital microscopy. Development. 1995; 121:935–45. [PubMed: 7743937]

Brown CB, Feiner L, Lu MM, Li J, Ma X, Webber AL, Jia L, Raper JA, Epstein JA. PlexinA2 and semaphorin signaling during cardiac neural crest development. Development. 2001; 128:3071–80. [PubMed: 11688557]

Brugger SM, Merrill AE, Torres-Vazquez J, Wu N, Ting MC, Cho JYM, Dobias SL, Yi SE, Lyons K, Bell JR, Arora K, Warrior R, Maxson R. A phylogenetically conserved cis-regulatory module in the Msx2 promoter is sufficient for BMP-dependent transcription in murine and Drosophila embryos. Development. 2004; 131:5153–65. [PubMed: 15459107]

Chen Y, Bei M, Woo I, Satokata I, Maas R. Msx1 controls inductive signaling in mammalian tooth morphogenesis. Development. 1996; 122:3035–44. [PubMed: 8898217]

Chen Y, Zhang Y, Jiang TX, Barlow AJ, St Amand TR, Hu Y, Heaney S, Francis-West P, Chuong CM, Maas R. Conservation of early odontogenic signaling pathways in Aves. Proc Natl Acad Sci U S A. 2000; 97:10044–10049. [PubMed: 10954731]

Condie BG, Bain G, Gottlieb DI, Capecchi MR. Cleft palate in mice with a targeted mutation in the gamma-aminobutyric acid-producing enzyme glutamic acid decarboxylase 67. Proc Natl Acad Sci U S A. 1997; 94:11451–11455. [PubMed: 9326630]

Deng C, Zhang P, Harper JW, Elledge SJ, Leder P. Mice lacking p21CIP1/WAF1 undergo normal development, but are defective in G1 checkpoint control. Cell. 1995; 82:675–684. [PubMed: 7664346]

Dodig M, Tadic T, Kronenberg MS, Dacic S, Liu YH, Maxson R, Rowe DW, Lichtler AC. Ectopic Msx2 overexpression inhibits and Msx2 antisense stimulates calvarial osteoblast differentiation. Dev Biol. 1999; 209:298–307. [PubMed: 10328922]

Ellies DL, Tucker AS, Lumsden A. Apoptosis of Premigratory Neural Crest Cells in Rhombomeres 3 and 5: Consequences for Patterning of the Branchial Region. Dev Biol. 2002; 251:118–128. [PubMed: 12413902]

Engleka KA, Gitler AD, Zhang M, Zhou DD, High FA, Epstein JA. Insertion of Cre into the Pax3 locus creates a new allele of Splotch and identifies unexpected Pax3 derivatives. Dev Biol. 2005; 280:396–406. [PubMed: 15882581]

Feng D, Liu T, Sun Z, Bugge A, Mullican SE, Alenghat T, Liu XS, Lazar MA. A circadian rhythm orchestrated by histone deacetylase 3 controls hepatic lipid metabolism. Science. 2011; 331:1315–9. [PubMed: 21393543]

Gans C, Northcutt RG. Neural crest and the origin of vertebrates: a new head. Science. 1983; 220:268–273. [PubMed: 17732898]

Graham A, Heyman I, Lumsden A. Even-numbered rhombomeres control the apoptotic elimination of neural crest cells from odd-numbered rhombomeres in the chick hindbrain. Development. 1993; 119:233–45. [PubMed: 8275859]

Graham A, Francis-West P, Brickell P, Lumsden A. The signalling molecule BMP4 mediates apoptosis in the rhombencephalic neural crest. Nature. 1994; 372:684–686. [PubMed: 7990961]

Han J, Ishii M, Bringas P, Maas RL, Maxson RE, Chai Y. Concerted action of Msx1 and Msx2 in regulating cranial neural crest cell differentiation during frontal bone development. Mech Dev. 2007; 124:729–45. [PubMed: 17693062]

He F, Xiong W, Wang Y, Matsui M, Yu X, Chai Y, Klingensmith J, Chen Y. Modulation of BMP signaling by Noggin is required for the maintenance of palatal epithelial integrity during palatogenesis. Dev Biol. 2010; 347:109–121. [PubMed: 20727875]

He F, Xiong W, Wang Y, Li L, Liu C, Yamagami T, Taketo MM, Zhou C, Chen Y. Epithelial Wnt/beta-catenin signaling regulates palatal shelf fusion through regulation of Tgfbeta3 expression. Dev Biol. 2011; 350:511–519. [PubMed: 21185284]

Heidt AB, Black BL. Transgenic mice that express Cre recombinase under control of a skeletal muscle-specific promoter from mef2c. Genesis. 2005; 42:28–32. [PubMed: 15828002]

Hesse E, Saito H, Kiviranta R, Correa D, Yamana K, Neff L, Toben D, Duda G, Atfi A, Geoffroy V, Horne WC, Baron R. Zfp521 controls bone mass by HDAC3-dependent attenuation of Runx2 activity. J Cell Biol. 2010; 191:1271–1283. [PubMed: 21173110]

High FA, Lu MM, Pear WS, Loomes KM, Kaestner KH, Epstein JA. Endothelial expression of the Notch ligand Jagged1 is required for vascular smooth muscle development. Proc Natl Acad Sci U S A. 2008; 105:1955–1959. [PubMed: 18245384]

Hussein SM, Duff EK, Sirard C. Smad4 and beta-catenin co-activators functionally interact with lymphoid-enhancing factor to regulate graded expression of Msx2. J Biol Chem. 2003; 278:48805–14. [PubMed: 14551209]

Ishii M, Merrill AE, Chan YS, Gitelman I, Rice DPC, Sucov HM, Maxson RE. Msx2 and Twist cooperatively control the development of the neural crest-derived skeletogenic mesenchyme of the murine skull vault. Development. 2003; 130:6131–42. [PubMed: 14597577]

Ito Y, Yeo JY, Chytil A, Han J, Bringas P Jr, Nakajima A, Shuler CF, Moses HL, Chai Y. Conditional inactivation of Tgfbr2 in cranial neural crest causes cleft palate and calvaria defects. Development. 2003; 130:5269–5280. [PubMed: 12975342]

Ivens A, Flavin N, Williamson R, Dixon M, Bates G, Buckingham M, Robert B. The human homeobox gene HOX7 maps to chromosome 4p16.1 and may be implicated in Wolf-Hirschhorn syndrome. Hum Genet. 1990; 84:473–6. [PubMed: 1969845]

Jabs EW, Müller U, Li X, Ma L, Luo W, Haworth IS, Klisak I, Sparkes R, Warman ML, Mulliken JB. A mutation in the homeodomain of the human MSX2 gene in a family affected with autosomal dominant craniosynostosis. Cell. 1993; 75:443–50. [PubMed: 8106171]

Jain R, Engleka KA, Rentschler SL, Manderfield LJ, Li L, Yuan L, Epstein JA. Cardiac neural crest orchestrates remodeling and functional maturation of mouse semilunar valves. J Clin Invest. 2011; 121:422–30. [PubMed: 21157040]

Jiang X, Rowitch DH, Soriano P, McMahon AP, Sucov HM. Fate of the mammalian cardiac neural crest. Development. 2000; 127:1607–1616. [PubMed: 10725237]

Kollar EJ, Baird GR. The influence of the dental papilla on the development of tooth shape in embryonic mouse tooth germs. J Embryol Exp Morphol. 1969; 21:131–48. [PubMed: 5765787]

Köntges G, Lumsden A. Rhombencephalic neural crest segmentation is preserved throughout craniofacial ontogeny. Development. 1996; 122:3229–42. [PubMed: 8898235]

Lallemand Y, Nicola MA, Ramos C, Bach A, Clement CS, Robert B. Analysis of Msx1; Msx2 double mutants reveals multiple roles for Msx genes in limb development. Development. 2005; 132:3003–3014. [PubMed: 15930102]

Lan Y, Ovitt CE, Cho ES, Maltby KM, Wang Q, Jiang R. Odd-skipped related 2 (Osr2) encodes a key intrinsic regulator of secondary palate growth and morphogenesis. Development. 2004; 131:3207–16. [PubMed: 15175245]

Le Douarin, N. The neural crest. Cambridge Univ Press; 1982.

Liu YH, Ma L, Wu LY, Luo W, Kundu R, Sangiorgi F, Snead ML, Maxson R. Regulation of the Msx2 homeobox gene during mouse embryogenesis: a transgene with 439 bp of 5′ flanking sequence is expressed exclusively in the apical ectodermal ridge of the developing limb. Mech Dev. 1994; 48:187–97. [PubMed: 7893602]

Liu YH, Kundu R, Wu L, Luo W, Ignelzi MA Jr, Snead ML, Maxson RE Jr. Premature suture closure and ectopic cranial bone in mice expressing Msx2 transgenes in the developing skull. Proc Natl Acad Sci U S A. 1995; 92:6137–6141. [PubMed: 7597092]

Lumsden AG. Spatial organization of the epithelium and the role of neural crest cells in the initiation of the mammalian tooth germ. Development. 1988; 103(Suppl):155–69. [PubMed: 3250849]

Maas R, Bei M. The genetic control of early tooth development. Crit Rev Oral Biol Med. 1997; 8:4–39. [PubMed: 9063623]

Marazzi G, Wang Y, Sassoon D. Msx2 is a transcriptional regulator in the BMP4-mediated programmed cell death pathway. Dev Biol. 1997; 186:127–138. [PubMed: 9205134]

Mesbah K, Rana MS, Francou A, van Duijvenboden K, Papaioannou VE, Moorman AF, Kelly RG, Christoffels VM. Identification of a Tbx1/Tbx2/Tbx3 genetic pathway governing pharyngeal and arterial pole morphogenesis. Hum Mol Genet. 2012; 21:1217–29. [PubMed: 22116936]

Mina M, Kollar EJ. The induction of odontogenesis in non-dental mesenchyme combined with early murine mandibular arch epithelium. Arch Oral Biol. 1987; 32:123–7. [PubMed: 3478009]

Mitsiadis TA, Graf D, Luder H, Gridley T, Bluteau G. BMPs and FGFs target Notch signalling via jagged 2 to regulate tooth morphogenesis and cytodifferentiation. Development. 2010; 137:3025–35. [PubMed: 20685737]

Mullican SE, Gaddis CA, Alenghat T, Nair MG, Giacomin PR, Everett LJ, Feng D, Steger DJ, Schug J, Artis D, Lazar MA. Histone deacetylase 3 is an epigenomic brake in macrophage alternative activation. Genes Dev. 2011; 25:2480–2488. [PubMed: 22156208]

Novak A, Guo C, Yang W, Nagy A, Lobe CG. Z/EG, a double reporter mouse line that expresses enhanced green fluorescent protein upon Cre-mediated excision. Genesis. 2000; 28:147–155. [PubMed: 11105057]

Park K, Kim K, Rho SB, Choi K, Kim D, Oh S, Park J, Lee SH, Lee J. Homeobox Msx1 interacts with p53 tumor suppressor and inhibits tumor growth by inducing apoptosis. Cancer Res. 2005; 65:749–57. [PubMed: 15705871]

Qiu M, Bulfone A, Martinez S, Meneses JJ, Shimamura K, Pedersen RA, Rubenstein JL. Null mutation of Dlx-2 results in abnormal morphogenesis of proximal first and second branchial arch

derivatives and abnormal differentiation in the forebrain. Genes Dev. 1995; 9:2523–2538. [PubMed: 7590232]

Razidlo DF, Whitney TJ, Casper ME, McGee-Lawrence ME, Stensgard BA, Li X, Secreto FJ, Knutson SK, Hiebert SW, Westendorf JJ. Histone deacetylase 3 depletion in osteo/chondroprogenitor cells decreases bone density and increases marrow fat. PLoS One. 2010; 5:e11492. [PubMed: 20628553]

Richarte AM, Mead HB, Tallquist MD. Cooperation between the PDGF receptors in cardiac neural crest cell migration. Dev Biol. 2007; 306:785–796. [PubMed: 17499702]

Roybal PG, Wu NL, Sun J, Ting MC, Schafer CA, Maxson RE. Inactivation of Msx1 and Msx2 in neural crest reveals an unexpected role in suppressing heterotopic bone formation in the head. Dev Biol. 2010; 343:28–39. [PubMed: 20398647]

Santagati F, Rijli FM. Cranial neural crest and the building of the vertebrate head. Nat Rev Neurosci. 2003; 4:806–818. [PubMed: 14523380]

Satokata I, Maas R. Msx1 deficient mice exhibit cleft palate and abnormalities of craniofacial and tooth development. Nat Genet. 1994; 6:348–56. [PubMed: 7914451]

Satokata I, Ma L, Ohshima H, Bei M, Woo I, Nishizawa K, Maeda T, Takano Y, Uchiyama M, Heaney S, Peters H, Tang Z, Maxson R, Maas R. Msx2 deficiency in mice causes pleiotropic defects in bone growth and ectodermal organ formation. Nat Genet. 2000; 24:391–5. [PubMed: 10742104]

Sauka-Spengler T, Bronner-Fraser M. A gene regulatory network orchestrates neural crest formation. Nat Rev Mol Cell Biol. 2008; 9:557–568. [PubMed: 18523435]

Schroeder TM, Kahler RA, Li X, Westendorf JJ. Histone deacetylase 3 interacts with runx2 to repress the osteocalcin promoter and regulate osteoblast differentiation. J Biol Chem. 2004; 279:41998–42007. [PubMed: 15292260]

Sechrist J, Serbedzija GN, Scherson T, Fraser SE, Bronner-Fraser M. Segmental migration of the hindbrain neural crest does not arise from its segmental generation. Development. 1993; 118:691–703. [PubMed: 7521280]

Sharpe J, Ahlgren U, Perry P, Hill B, Ross A, Hecksher-Sorensen J, Baldock R, Davidson D. Optical projection tomography as a tool for 3D microscopy and gene expression studies. Science. 2002; 296:541–545. [PubMed: 11964482]

Singh N, Trivedi CM, Lu M, Mullican SE, Lazar MA, Epstein JA. Histone deacetylase 3 regulates smooth muscle differentiation in neural crest cells and development of the cardiac outflow tract. Circ Res. 2011; 109:1240–1249. [PubMed: 21959220]

Takahashi T, Guron C, Shetty S, Matsui H, Raghow R. A minimal murine Msx-1 gene promoter. Organization of its cis-regulatory motifs and their role in transcriptional activation in cells in culture and in transgenic mice. J Biol Chem. 1997; 272:22667–78. [PubMed: 9278425]

Tríbulo C, Aybar MJ, Sánchez SS, Mayor R. A balance between the anti-apoptotic activity of Slug and the apoptotic activity of msx1 is required for the proper development of the neural crest. Dev Biol. 2004; 275:325–42. [PubMed: 15501222]

Trivedi CM, Lu MM, Wang Q, Epstein JA. Transgenic overexpression of Hdac3 in the heart produces increased postnatal cardiac myocyte proliferation but does not induce hypertrophy. J Biol Chem. 2008; 283:26484–26489. [PubMed: 18625706]

Vallejo-Illarramendi A, Zang K, Reichardt LF. Focal adhesion kinase is required for neural crest cell morphogenesis during mouse cardiovascular development. J Clin Invest. 2009; 119:2218–2230. [PubMed: 19587446]

Wang Z, Zang C, Cui K, Schones DE, Barski A, Peng W, Zhao K. Genome-wide mapping of HATs and HDACs reveals distinct functions in active and inactive genes. Cell. 2009; 138:1019–31. [PubMed: 19698979]

Warman ML, Mulliken JB, Hayward PG, Müller U. Newly recognized autosomal dominant disorder with craniosynostosis. Am J Med Genet. 1993; 46:444–9. [PubMed: 8357019]

Wilson AJ, Byun DS, Nasser S, Murray LB, Ayyanar K, Arango D, Figueroa M, Melnick A, Kao GD, Augenlicht LH, Mariadason JM. HDAC4 promotes growth of colon cancer cells via repression of p21. Mol Biol Cell. 2008; 19:4062–4075. [PubMed: 18632985]

Winograd J, Reilly MP, Roe R, Lutz J, Laughner E, Xu X, Hu L, Asakura T, vander Kolk C, Strandberg JD, Semenza GL. Perinatal lethality and multiple craniofacial malformations in MSX2 transgenic mice. Hum Mol Genet. 1997; 6:369–379. [PubMed: 9147639]

Wu M, Li J, Engleka KA, Zhou B, Lu MM, Plotkin JB, Epstein JA. Persistent expression of Pax3 in the neural crest causes cleft palate and defective osteogenesis in mice. J Clin Invest. 2008; 118:2076–2087. [PubMed: 18483623]

You SH, Lim HW, Sun Z, Broache M, Won KJ, Lazar MA. Nuclear receptor co-repressors are required for the histone-deacetylase activity of HDAC3 in vivo. Nat Struct Mol Biol. 2013; 3:1–7.

Yu L, Gu S, Alappat S, Song Y, Yan M, Zhang X, Zhang G, Jiang Y, Zhang Z, Zhang Y, Chen Y. Shox2-deficient mice exhibit a rare type of incomplete clefting of the secondary palate. Development. 2005; 132:4397–406. [PubMed: 16141225]

Zhang Z, Song Y, Zhao X, Zhang X, Fermin C, Chen Y. Rescue of cleft palate in Msx1-deficient mice by transgenic Bmp4 reveals a network of BMP and Shh signaling in the regulation of mammalian palatogenesis. Development. 2002; 129:4135–46. [PubMed: 12163415]

Zirzow S, Ludtke TH, Brons JF, Petry M, Christoffels VM, Kispert A. Expression and requirement of T-box transcription factors Tbx2 and Tbx3 during secondary palate development in the mouse. Dev Biol. 2009; 336:145–155. [PubMed: 19769959]

Research Highlights

- Loss of *Hdac3* in neural crest results in severe craniofacial malformations
- Cleft palate in *Hdac3* mutants results from reduced palatal shelf expansion
- Mutants have higher expression of cell cycle regulators in neural crest derivatives
- *Hdac3* deletion in neural crest results in higher expression of Msx1, Msx2 and Bmp4

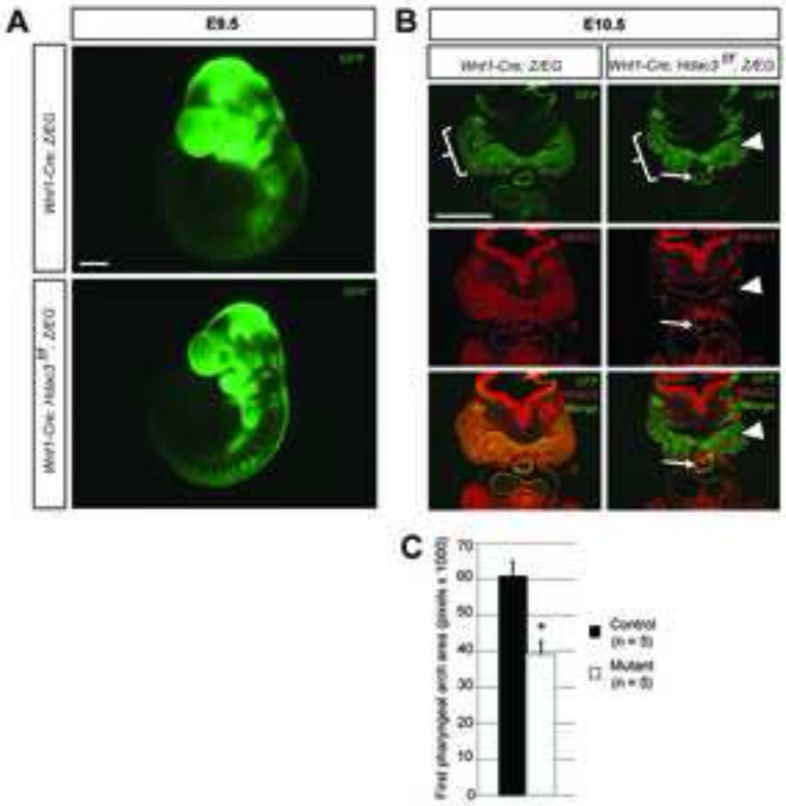

Fig. 1. Deletion of Hdac3 in neural crest results in cranial hypoplasia at E10.5

(A) Gross images of E9.5 embryos visualized with direct fluorescence. Migration of neural crest cells into the developing face and pharyngeal arch region is grossly intact in the absence of neural crest expression of Hdac3. (B) Immunohistochemistry for GFP and Hdac3 in frontal sections of the facial mesenchyme of E10.5 embryos. *Hdac3* is efficiently deleted in neural crest-derived cranial mesenchyme (arrowhead), as well as the conotruncal cushions of the developing cardiac outflow tract (arrow). Note that cranial crest-derived (GFP+) structures in the mutant are hypoplastic (open bracket). (C) Quantification of the size of the first pharyngeal arch from serial sections of E10.5 control and mutant embryos. Scale bars: (A): 300μm. (B): 400μm.

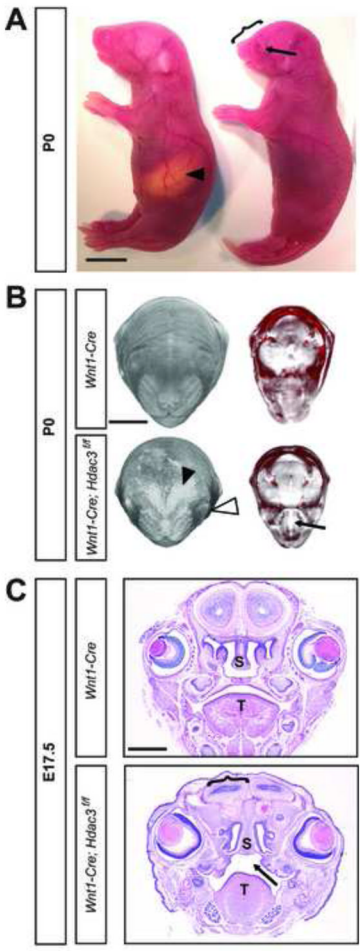

Fig. 2. Craniofacial abnormalities in *Hdac3*^{Wnt1NCKO} mice

(A) Gross image of a control (left) and mutant P0 pup. Mutants have severe cranial hypoplasia, characterized by a shortened snout (bracket) and micrognathia, and are unable to feed, as indicated by the absence of a milk spot, present in littermate controls (arrowhead). Mutants also exhibit eyelid dysplasia (arrow). (B) Optical projection tomography renderings of P0 heads. (Left panels) Viewed *en face*, an area of hemorrhage (black arrowhead) and eyelid closure defects (white arrowhead) are visible in the mutant. (Right panels) Virtual transverse sections cut through the level of the eyes demonstrate a cleft palate (arrow) in the mutant. (C) H&E stained coronal sections of E17.5 heads. Cleft palate is indicated by the arrow. S: Nasal septum. T: Tongue. Scale bars: (A): 500μm. (B): 2mm. (C): 1.4mm.

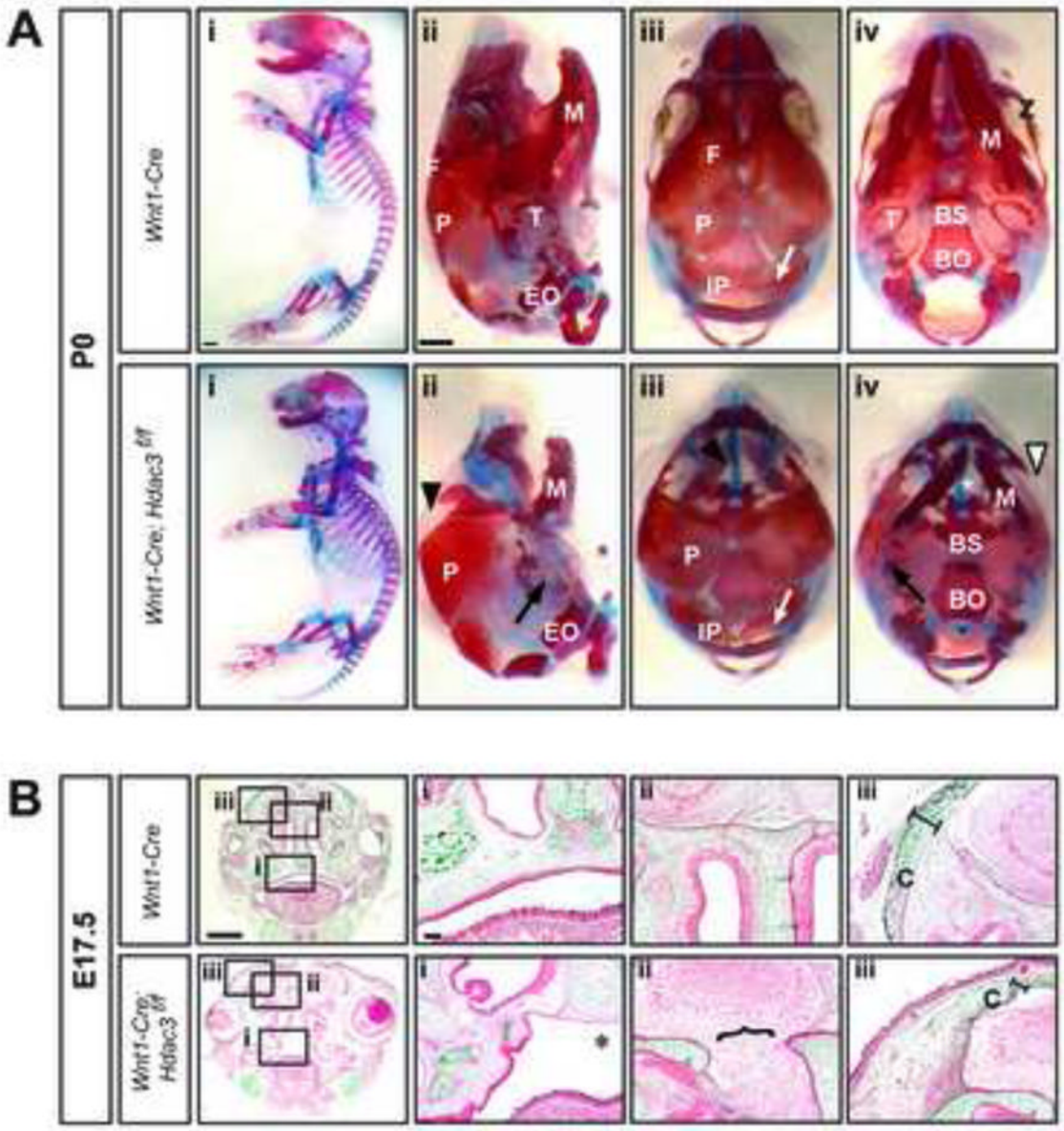

Fig. 3. *Hdac3*^{Wnt1NCKO} embryos exhibit defects in craniofacial bone formation

(A) Alcian blue and alizarin red staining of P0 heads. Red staining indicates ossified bone, blue staining indicates cartilage. (Inset i) Lateral view of the full skeleton. (Inset ii) Lateral view of the calvaria. (Inset iii) Caudal view of the calvaria. (Inset iv) Rostral view of the skull base. Mutants demonstrate absence of the tympanic ring (T) (black arrow), diminished ossification of the frontal bone (F) (black arrowhead), absence of the ossified secondary palate (SP) (asterisk), and decreased mineralization along the midline of the interparietal bone (IP) (white arrow). Mutants also exhibit hypoplasia and decreased ossification of neural crest-derived viscerocranial structures, including the zygomatic arch (Z) (white arrowhead). Ossification of the mesodermally-derived parietal bone (P) remains intact. (B) Goldner's trichrome staining of E17.5 heads. Green staining represents bone, red staining represents connective tissues. (Inset i) Asterisk indicates cleft palate in the mutant. (Inset ii) Open bracket indicates an area of brain herniating through the base of the skull in the mutant. (Inset iii) Decreased ossification of the calvaria (C) in the mutant, as indicated by a

black bar. BO: Basioccipital. BS: Basisphenoid. EO: Exoccipital. IP: Intraparietal. M. Mandible. N. Nasal. Scale bars: (A): 1mm. (B): 1.4mm.

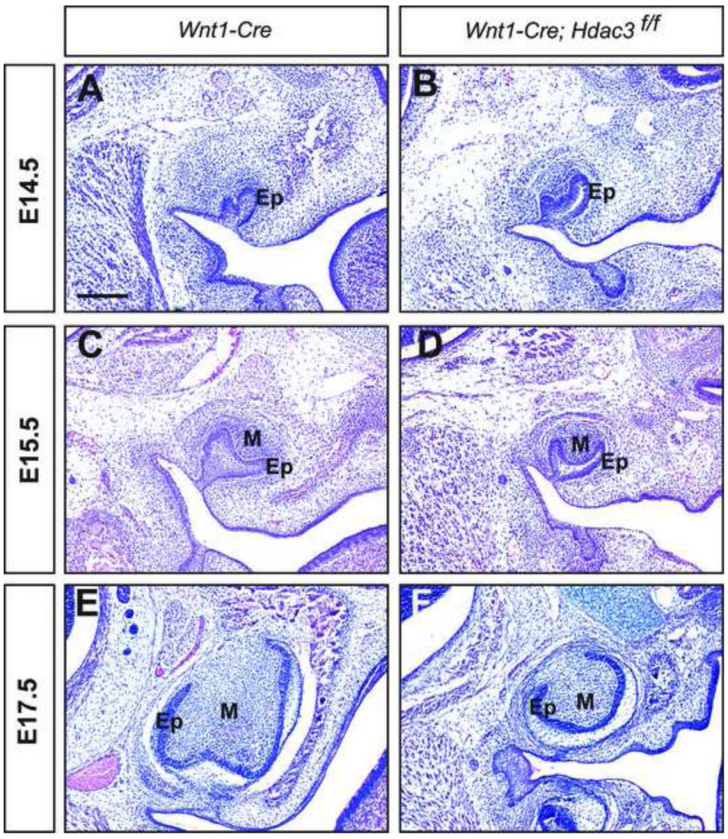

Fig. 4. The loss of Hdac3 causes hypoplasia of neural crest-derived dental mesenchyme

(A–F) H & E stained frontal sections of control and mutant heads at E17.5. Early stages of tooth morphogenesis, including epithelial invagination (A, B) and mesenchymal specification (C, D) occur normally in the absence of *Hdac3*. (E, F) However, at E17.5, the dental pulp shows decreased bulk in mutants. Ep: Epithelium. M: mesenchyme. Scale bar: (A–F) 200μm.

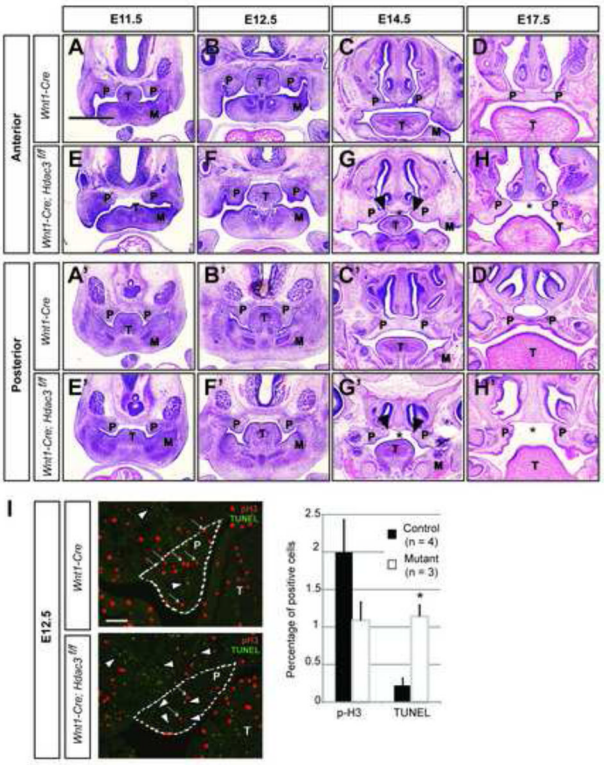

Fig. 5. Cleft palate in *Hdac3*^{Wnt1NCKO} mice results from increased apoptosis in the neural crest-derived palatal shelves

(A–H,A′–H′) H&E stained frontal sections of control and mutant embryos at the level of the anterior and posterior palatal shelves. (A–D,A′–D′) In control embryos, the palatal shelves (P) expand towards the mandible (M) before elevating above the tongue (T), meeting in the midline at E14.5 and ossifying by E17.5. (E–H,E′–H′) In mutant embryos, the palatal shelves are hypoplastic at E12.5 and do not meet in the midline at E14.5 (*), although the medial aspects of the palatal shelves do elevate above the tongue (arrowheads). (I) Images show the areas defined as palatal shelves in control and mutant embryos at E12.5. Phospho-histone H3 (pH3)- (arrows) and TUNEL- (arrowheads) positive nuclei were counted relative to total nuclei in serial sections of the pharyngeal arch mesenchyme. Asterisk denotes $p < 0.05$. Scale bars: (A–H,A′–H′): 400μm. (I): 50μm.

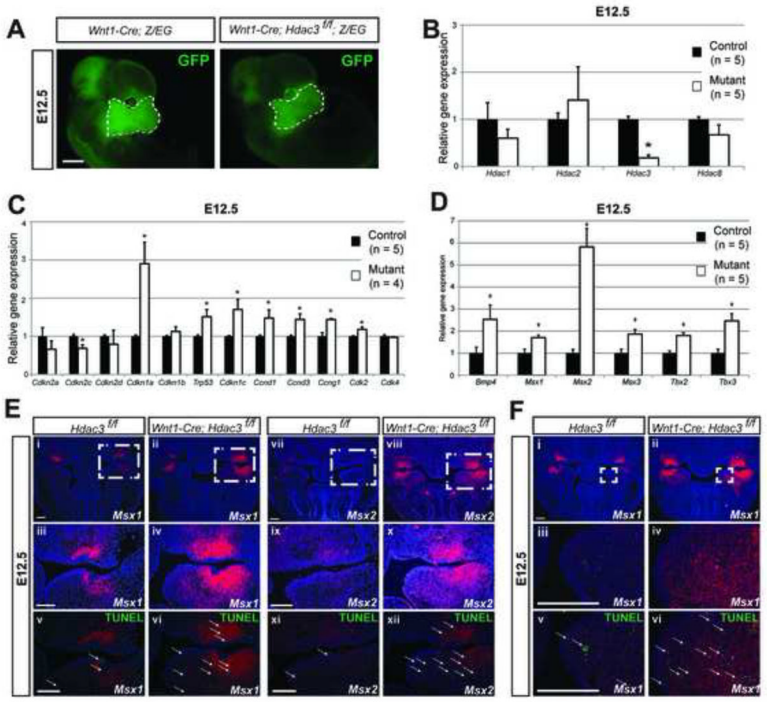

Fig. 6. Dysregulation of cell cycle genes and the Msx-Bmp4 apoptotic pathway in *Hdac3*^{Wnt1NCKO} cranial mesenchyme

(A) Representative fluorescent images showing the area of cranial mesenchyme microdissected for E12.5 expression profiling. (B–D) Quantitative RT-PCR results. (B) Expression of *Hdac3*, but not other class I Hdacs, is decreased in mutant tissue. (C) Mutant cranial mesenchyme exhibit significant dysregulation of cell cycle regulatory genes. (D) Among important regulatory genes involved in craniofacial development, *Bmp4, Msx* and *Tbx* expression are significantly altered. (E,F) *In situ* hybridization of *Msx1*and *Msx2* in transverse sections of E12.5 heads and TUNEL staining. (E) Expression of *Msx1* transcripts is increased in mutant dental mesenchyme (Insets ii, iv) compared to littermate control (Insets i, iii). Expression of *Msx2* transcripts is increased in mutant dental mesenchyme (Insets viii, x) compared to littermate control (Insets vii, ix). TUNEL staining (Insets v, vi, xi, xii) of adjacent sections merged with images of *Msx* expression reveals increased apoptosis in mutant versus control embryos in the areas of higher *Msx* expression (arrows). (F) Expression of *Msx1* transcripts is increased in mutant palatal shelves (Insets ii, iv) compared to littermate control (Insets i, iii), as well as apoptosis labeled by TUNEL staining of adjacent sections (Insets v, vi) (arrows). (*) denotes $p < 0.05$. Scale bars: (A): 150μm. (E, F): 200μm.

Table 1

Late gestation and perinatal craniofacial abnormalities in *Hdac3*^{Wnt1NCKO} mice.

E16.5-P0	***Wnt1-Cre***	***Wnt1-Cre; Hdac3*$^{f/f}$**
Microcephaly	0% (0/20)	100% (27/27)
Cleft palate	0% (0/20)	100% (27/27)
Eyelid dysplasia	0% (0/20)	100% (27/27)
Anteriorally displaced foramen magnum	0% (0/20)	100% (27/27)
Absence of:		
Hyoid bone	0% (0/7)	75% (6/8)
Sphenoid bone	0% (0/7)	88% (7/8)
Tympanic ring	0% (0/7)	88% (7/8)
Hypoplasia and incomplete mineralization of:		
Frontal bone	0% (0/7)	100% (8/8)
Mandible	0% (0/7)	100% (8/8)
Maxilla	0% (0/7)	100% (8/8)
Nasal bone	0% (0/7)	100% (8/8)
Orbit	0% (0/7)	100% (8/8)
Temporal bone	0% (0/7)	100% (8/8)
Zygomatic arch	0% (0/7)	100% (8/8)
Interparietal bone	0% (0/7)	100% (8/8)